

## Nature of Bonding in Terminal Borylene, Aylene, and Gallylene Complexes of Vanadium and Niobium $[(\eta^5\text{-C}_5\text{H}_5)(\text{CO})_3\text{M}(\text{ENR}_2)]$ ( $\text{M} = \text{V}, \text{Nb}$ ; $\text{E} = \text{B}, \text{Al}, \text{Ga}$ ; $\text{R} = \text{CH}_3, \text{SiH}_3, \text{CMe}_3, \text{SiMe}_3$ ): A DFT Study

Krishna K. Pandey,<sup>\*†</sup> Holger Braunschweig,<sup>\*‡</sup> and Agustí Lledós<sup>\*§</sup>

<sup>†</sup>School of Chemical Sciences, Devi Ahilya University Indore, Indore 452017, India,

<sup>‡</sup>Institut für Anorganische Chemie, Julius-Maximilians-Universität Würzburg, Am Hubland, D-97074 Würzburg, Germany, and <sup>§</sup>Departament de Química, Universitat Autònoma de Barcelona, 08193 Bellaterra, Barcelona, Spain

Received September 27, 2010

Density functional theory calculations have been performed for the terminal borylene, aylene, and gallylene complexes  $[(\eta^5\text{-C}_5\text{H}_5)(\text{CO})_3\text{M}(\text{ENR}_2)]$  ( $\text{M} = \text{V}, \text{Nb}$ ;  $\text{E} = \text{B}, \text{Al}, \text{Ga}$ ;  $\text{R} = \text{CH}_3, \text{SiH}_3, \text{CMe}_3, \text{SiMe}_3$ ) using the exchange correlation functional BP86. The calculated geometry parameters of vanadium borylene complex  $[(\eta^5\text{-C}_5\text{H}_5)(\text{CO})_3\text{V}\{\text{BN}(\text{SiMe}_3)_2\}]$  are in excellent agreement with their available experimental values. The  $\text{M}-\text{B}$  bonds in the borylene complexes have partial  $\text{M}-\text{B}$  double-bond character, and the  $\text{B}-\text{N}$  bonds are nearly  $\text{B}=\text{N}$  double bonds. On the other hand, the  $\text{M}-\text{E}$  bonds in the studied metal aylene and gallylene complexes represent  $\text{M}-\text{E}$  single bonds with a very small  $\text{M}-\text{E}$   $\pi$ -orbital contribution, and the  $\text{Al}-\text{N}$  and  $\text{Ga}-\text{N}$  bonds in the complexes have partial double-bond character. The orbital interactions between metal and  $\text{ENR}_2$  in  $[(\eta^5\text{-C}_5\text{H}_5)(\text{CO})_3\text{M}(\text{ENR}_2)]$  arise mainly from  $\text{M} \leftarrow \text{ENR}_2 \sigma$  donation. The  $\pi$ -bonding contribution is, in all complexes, much smaller. The contributions of the electrostatic interactions  $\Delta E_{\text{elstat}}$  are significantly larger in all borylene, aylene, and gallylene complexes than the covalent bonding  $\Delta E_{\text{orb}}$ ; that is, the  $\text{M}-\text{ENR}_2$  bonding in the complexes has a greater degree of ionic character.

### Introduction

Synthesis, structure, reactivity, and bonding in transition-metal borylene complexes have been a provocative subject since the first report of structurally characterized two-coordinate transition-metal borylene complexes in 1998.<sup>1,2</sup> So far, a number of structurally characterized terminal transition-metal

borylene complexes<sup>1–20</sup> have been reported (Table 1). Additionally, a number of base-stabilized adducts formed by coordination of a Lewis base (main group or transition metal) to the two- or three-coordinate boron center have also been reported.<sup>20–32</sup> The topic of borylene complexes has

- \*To whom correspondence should be addressed. E-mail: kkpandey.schem@dauniv.ac.in (K.K.P.), h.braunschweig@mail.uni-wuerzburg.de (H.B.), agusti@klingon.uab.cat (A.L.).  
(1) Braunschweig, H.; Kollann, C.; Englert, U. *Angew. Chem., Int. Ed.* **1998**, *37*, 3179.  
(2) Cowley, A. H.; Lomeli, V.; Voigt, A. *J. Am. Chem. Soc.* **1998**, *120*, 6401.  
(3) Braunschweig, H.; Colling, M.; Kollann, C.; Stammler, H. G.; Neumann, B. *Angew. Chem., Int. Ed.* **2001**, *40*, 2298.  
(4) Braunschweig, H.; Colling, M.; Kollann, C.; Merz, K.; Radacki, K. *Angew. Chem., Int. Ed.* **2001**, *40*, 4198.  
(5) Braunschweig, H.; Colling, M.; Hu, C.; Radacki, K. *Angew. Chem., Int. Ed.* **2003**, *42*, 205.  
(6) Braunschweig, H.; Radacki, K.; Rais, D.; Uttinger, K. *Angew. Chem., Int. Ed.* **2006**, *45*, 162.  
(7) Braunschweig, H.; Radacki, K.; Rais, D.; Uttinger, K. *Organometallics* **2006**, *25*, 5159.  
(8) Blank, B.; Colling-Hendelkens, M.; Kollann, C.; Radacki, K.; Rais, D.; Uttinger, K.; Whittell, G. R.; Braunschweig, H. *Chem.—Eur. J.* **2007**, *13*, 4770.  
(9) Braunschweig, H.; Burzler, M.; Kupfer, T.; Radacki, K.; Seeler, F. *Angew. Chem., Int. Ed.* **2007**, *46*, 7785.

- (10) Braunschweig, H.; Forster, M.; Kupfer, T.; Seeler, F. *Angew. Chem., Int. Ed.* **2008**, *47*, 5981.  
(11) Braunschweig, H.; Kupfer, T.; Radacki, K.; Schneider, A.; Seeler, F.; Uttinger, K.; Wu, H. *J. Am. Chem. Soc.* **2008**, *130*, 7974.  
(12) Alcaraz, G.; Helmstedt, U.; Clot, E.; Vendier, L.; Sabo-Etienne, S. *J. Am. Chem. Soc.* **2008**, *130*, 12878.  
(13) Coombs, D. L.; Aldridge, S.; Jones, C.; Willock, D. *J. J. Am. Chem. Soc.* **2003**, *125*, 6356.  
(14) Coombs, D. L.; Aldridge, S.; Rossin, A.; Jones, C.; Willock, D. *J. Organometallics* **2004**, *23*, 2911.  
(15) Aldridge, S.; Jones, C.; Gans-Eichler, T.; Stasch, A.; Kays, D. L.; Coombs, N. D.; Willock, D. *J. Angew. Chem., Int. Ed.* **2006**, *45*, 6118.  
(16) Vidovic, D.; Findlater, M.; Reeske, G.; Cowley, A. H. *Chem. Commun.* **2006**, 3786.  
(17) Braunschweig, H.; Radacki, K.; Uttinger, K. *Angew. Chem., Int. Ed.* **2007**, *46*, 3979.  
(18) Pierce, G. A.; Vidovic, D.; Kays, D. L.; Coombs, N. D.; Thompson, A. L.; Jemmis, E. D.; De, S.; Aldridge, S. *Organometallics* **2009**, *28*, 2947.  
(19) De, S.; Pierce, G. A.; Vidovic, D.; Kays, D. L.; Coombs, N. D.; Jemmis, E. D.; Aldridge, S. *Organometallics* **2009**, *28*, 2961.  
(20) Addy, D. A.; Pierce, G. A.; Vidovic, D.; Mallick, D.; Jemmis, E. D.; Goicoechea, J. M.; Aldridge, S. *J. Am. Chem. Soc.* **2010**, *132*, 4586.  
(21) Braunschweig, H. *Angew. Chem., Int. Ed.* **1998**, *37*, 1786.  
(22) Braunschweig, H.; Colling, M. *J. Organomet. Chem.* **2000**, *614–615*, 18.

**Table 1.** Selected Structurally Characterized Two-Coordinate Terminal Metal Borylene and Metal Gallylene Complexes

complex <sup>a</sup>	M–E (Å)	E–N/C (Å)	∠M–E–N/C (deg)
Transition-Metal Borylene Complexes			
$[(\eta^5\text{-C}_5\text{H}_5)(\text{CO})_3\text{V}\{\text{BN}(\text{SiMe}_3)_2\}]$	1.959(6)	1.378(7)	177.9(4)
$[(\text{CO})_5\text{Cr}\{\text{BN}(\text{SiMe}_3)_2\}]$	1.996(6)	1.353(6)	177.4(4)
$[(\text{CO})_5\text{Mo}\{\text{BN}(\text{SiMe}_3)_2\}]$	2.125(2)	1.355(2)	177.81(11)
$[(\text{CO})_5\text{W}\{\text{BN}(\text{SiMe}_3)_2\}]$	2.151(7)	1.338(8)	177.9(5)
$[(\text{Cy}_3\text{P})(\text{CO})_4\text{Cr}\{\text{BN}(\text{SiMe}_3)_2\}]$	1.915(2)	1.364(3)	175.91(16)
$[(\text{Cy}_3\text{P})(\text{CO})_4\text{Mo}\{\text{BN}(\text{SiMe}_3)_2\}]$	2.059(3)	1.365(3)	175.3(2)
$[(\text{Cy}_3\text{P})(\text{CO})_4\text{W}\{\text{BN}(\text{SiMe}_3)_2\}]$	2.058(6)	1.378(7)	175.8(5)
$[(\text{CO})_5\text{Cr}\{\text{BSi}(\text{SiMe}_3)_2\}]$	1.878(10)		
$[(\eta^5\text{-C}_5\text{H}_5)(\text{CO})_2\text{Mn}(\text{B}^1\text{Bu})]$	1.809(9)	1.531(11)	174.3(7)
$[(\text{Cy}_3\text{P})_2\text{HClRu}(\text{BMes})]$	1.780(4)	1.558(5)	178.1(3)
$[(\eta^5\text{-C}_5\text{Me}_5)(\text{CO})\text{Ir}\{\text{BN}(\text{SiMe}_3)_2\}]$	1.892(3)	1.365(4)	175.9(3)
$[(\eta^5\text{-C}_5\text{Me}_5)(\text{CO})_2\text{Fe}(\text{BMes})]^+$	1.792(8)	1.491(10)	178.3(6)
$[(\eta^5\text{-C}_5\text{Me}_5)(\text{CO})_2\text{Fe}(\text{BN}^1\text{Pr}_2)]^+$	1.835(3)	1.334(3)	
$[(\eta^5\text{-C}_5\text{Me}_5)(\text{CO})_2\text{Ru}(\text{BN}^1\text{Pr}_2)]^+$	1.950(8)	1.333(9)	
$[(\eta^5\text{-C}_5\text{Me}_5)(\text{CO})_2\text{Fe}(\text{BNCy}_3)]^+$	1.859(6)	1.324(7)	
$[(\eta^5\text{-C}_5\text{Me}_5)(\text{CO})_2\text{Fe}(\text{BNMe}_3)]^+$	1.811(3)	1.357(3)	
$[(\eta^5\text{-C}_5\text{Me}_5)(\text{CO})_2\text{Ru}(\text{BNCy}_3)]^+$	1.860(6)	1.320(7)	175.4(2)
$[(\eta^5\text{-C}_5\text{Me}_5)(\text{PMe}_3)((\text{CO})\text{Fe}(\text{BNCy}_3)]^+$	1.821(4)	1.347(5)	177.7(3)
$[(\eta^5\text{-C}_5\text{Me}_5)(\text{PMe}_3)((\text{CO})\text{Ru}(\text{BNCy}_3)]^+$	1.928(4)	1.345(5)	170.8(3)
<i>trans</i> - $[\text{Br}(\text{PCy}_3)_2\text{Pt}(\text{BMes})]^+$	1.859(3)	1.495(4)	178.15(9)
Transition-Metal Gallylene Complexes			
$[(\text{CO})_4\text{Fe}(\text{GaAr}^*)]$	2.2248(7)	1.943(3)	179.2(1)
$[(\eta^5\text{-C}_5\text{H}_5)\text{Ti}(\text{GaAr}^*)]$	2.4922(7)	2.025(3)	171.02(9)
$[(\eta^5\text{-C}_5\text{H}_5)\text{Zr}(\text{GaAr}^*)]$	2.6350(5)	2.003(5)	172.44(16)
$[(\eta^5\text{-C}_5\text{H}_5)\text{Hf}(\text{GaAr}^*)]$	2.6198(13)	2.021(10)	171.7(3)
$[\text{Ni}\{\text{GaC}(\text{SiMe}_3)_3\}_4]$	2.1700(4)	2.014(4)	180.00(5)
$[(\eta^5\text{-C}_5\text{Me}_5)(\text{dppe})\text{Fe}\{\text{GaFe}(\text{CO})_4\}]^b$	2.2479(10)		
$[(\eta^5\text{-C}_5\text{Me}_5)(\text{dppe})\text{Fe}\{\text{GaW}(\text{CO})_5\}]^b$	2.2687(12)		
$[(\eta^5\text{-C}_5\text{Me}_5)(\text{dppe})\text{Fe}\{\text{GaFe}(\text{CO})_3(\text{P}(\text{OPh})_3)\}]^c$	2.2690(8)		
$[(\eta^5\text{-C}_5\text{Me}_5)(\text{dppe})\text{Fe}\{\text{GaGe}(\text{CO})_3(\text{PMe}_3)\}]^d$	2.2769(5)		
$\{(\eta^5\text{-C}_5\text{Me}_5)\text{Ga}\}_4\text{Rh}(\text{GaCH}_3)]^+$	2.4711(10)	1.958(11)	176.1(5)
$[(\eta^5\text{-C}_5\text{Me}_5)(\text{dppe})\text{Fe}(\text{Gal})]^e$	2.2221(6)		

<sup>a</sup> Ar\* =  $-\text{C}_6\text{H}_3\text{--}2\text{,}6\text{-(2,4,6-}^{\text{i}}\text{Pr}_3\text{C}_6\text{H}_2\text{)}_2$ . <sup>b</sup> dppe = diphenylphosphineethane;  $\angle \text{Fe}-\text{Ga}-\text{Fe} = 176.01(4)^\circ$ ;  $\angle \text{Fe}-\text{Ga}-\text{W} = 173.78(4)^\circ$ . <sup>c</sup>  $\angle \text{Fe}-\text{Ga}-\text{Fe} = 176.430(12)^\circ$ . <sup>d</sup>  $\angle \text{Fe}-\text{Ga}-\text{Fe} = 177.389(19)^\circ$ . <sup>e</sup> Ga–I = 2.4436(5) Å;  $\angle \text{Fe}-\text{Ga}-\text{I} = 171.37(3)^\circ$ .

been covered by a range of review articles in recent years.<sup>32,33</sup> In contrast to transition-metal borylene complexes, relatively

- (23) Braunschweig, H.; Colling, M. *Coord. Chem. Rev.* **2001**, 223, 1.
- (24) Braunschweig, H.; Colling, M. *Eur. J. Inorg. Chem.* **2003**, 393.
- (25) Braunschweig, H. *Adv. Organomet. Chem.* **2004**, 51, 163.
- (26) Braunschweig, H.; Rais, D. *Heteroat. Chem.* **2005**, 16, 566.
- (27) Braunschweig, H.; Kollann, C.; Rais, D. *Angew. Chem., Int. Ed.* **2006**, 45, 5254.
- (28) Braunschweig, H.; Kollann, C.; Seeler, F. *Struct. Bonding (Berlin)* **2008**, 130, 1.
- (29) Anderson, C. E.; Braunschweig, H.; Dewhurst, R. D. *Organometallics* **2008**, 27, 6381.
- (30) Braunschweig, H.; Dewhurst, R. D. *Angew. Chem., Int. Ed.* **2009**, 48, 1893.
- (31) Braunschweig, H.; Dewhurst, R. D. *Angew. Chem., Int. Ed.* **2010**, 49, 3412.
- (32) Braunschweig, H.; Dewhurst, R. D.; Schneider, A. *Chem. Rev.* **2010**, 110, 3924.
- (33) Vidovic, D.; Pierce, G. A.; Aldridge, S. *Chem. Commun.* **2009**, 1157.
- (34) Su, J. R.; Li, X.-W.; Crittendon, R. C.; Campana, C. F.; Robinson, G. H. *Organometallics* **1997**, 16, 4511.
- (35) Yang, X.-J.; Quillian, B.; Wang, Y. Z.; Wei, P. R.; Robinson, G. H. *Organometallics* **2004**, 23, 5119.
- (36) Yang, X.-J.; Wang, Y. Z.; Quillian, B.; Wei, P. R.; Chen, Z.; Schleyer, P. v. R.; Robinson, G. H. *Organometallics* **2006**, 25, 925.
- (37) Quillian, P.; Wang, Y.; Wei, P.; Robinson, G. H. *New J. Chem.* **2008**, 32, 774.
- (38) Uhl, W.; Benter, M.; Melle, S.; Saak, W.; Frenking, G.; Uddin, J. *Organometallics* **1999**, 18, 3778.
- (39) Ueno, K.; Watanabe, T.; Tobita, H.; Ogino, H. *Organometallics* **2003**, 22, 4375.
- (40) Muraoka, T.; Motohashi, H.; Hirotsu, M.; Ueno, K. *Organometallics* **2008**, 27, 3918.
- (41) Muraoka, T.; Motohashi, H.; Kazuie, Y.; Takizawa, A.; Ueno, K. *Organometallics* **2009**, 28, 1616.

few transition-metal gallylene complexes are known.<sup>34–44</sup> To the best of our knowledge, no two-coordinate transition-metal alylene complex has been reported. In the literature, several transition-metal complexes with ligands Al( $\eta^5\text{-C}_5\text{R}_5$ ) and Ga( $\eta^5\text{-C}_5\text{R}_5$ ) have been reported by Fischer, Schnöckel, and co-workers.<sup>45–50</sup> These complexes may be considered as metal alane and metal gallane complexes, respectively, rather than metal alylene and metal gallylene complexes.

A number of theoretical studies of terminal metal borylene, alylene, and gallylene complexes have been reported.<sup>51–64</sup>

- (42) Coombs, N. D.; Clegg, W.; Thompson, A. L.; Wilcock, D. J.; Aldridge, S. *J. Am. Chem. Soc.* **2008**, 130, 5449.
- (43) Coombs, N. D.; Vidovic, D.; Day, J. K.; Thompson, A. L.; Le Pevelen, D. D.; Stasch, A.; Clegg, W.; Russo, L.; Male, L.; Hursthorne, M. B.; Wilcock, D. J.; Aldridge, S. *J. Am. Chem. Soc.* **2008**, 130, 16111.
- (44) Cadenbach, T.; Gemel, C.; Zacher, D.; Fischer, R. A. *Angew. Chem., Int. Ed.* **2008**, 47, 3438.
- (45) Weiss, J.; Setzkamp, D.; Nuber, B.; Fischer, R. A.; Boehme, C.; Frenking, G. *Angew. Chem., Int. Ed.* **1997**, 36, 70.
- (46) Yu, Q.; Purath, A.; Donchev, A.; Schnöckel, H. *J. Organomet. Chem.* **1999**, 584, 94.
- (47) Buchin, B.; Steinke, T.; Gemel, C.; Cadenbach, T.; Fischer, R. A. *Z. Anorg. Allg. Chem.* **2005**, 631, 2756.
- (48) Steinke, T.; Gemel, C.; Winter, M.; Fischer, R. A. *Chem.—Eur. J.* **2005**, 11, 1636.
- (49) Cadenbach, T.; Gemel, C.; Bollermann, T.; Fischer, R. A. *Inorg. Chem.* **2009**, 48, 5021 and references cited therein.
- (50) Cadenbach, T.; Gemel, C.; Schmid, R.; Halbherr, M.; Yusenko, K.; Cokoja, M.; Fischer, R. A. *Angew. Chem., Int. Ed.* **2009**, 48, 3872.
- (51) Ehlers, A. W.; Baerends, E. J.; Bickelhaupt, F. M.; Radius, U. *Chem.—Eur. J.* **1998**, 4, 210.

To the best of our knowledge, a bonding-energy analysis of terminal metal borylene, alylene, and galllyene complexes of vanadium and niobium has never been done before. A representative example of vanadium borylene complex  $[(\eta^5\text{-C}_5\text{H}_5)\text{-}(\text{CO})_3\text{V}\{\text{BN}(\text{SiMe}_3)_2\}]$  was reported by Braunschweig and co-workers.<sup>5</sup> We decided to investigate the nature of M=E bonds in the terminal metal borylene, alylene and galllyene complexes of vanadium and niobium with energy decomposition analysis (EDA).

In this paper, 16 neutral terminal borylene, alylene, and galllyene complexes of vanadium and niobium,  $[(\eta^5\text{-C}_5\text{H}_5)\text{-}(\text{CO})_3\text{M}(\text{ENR}_2)]$  (M = V, Nb; E = B, Al, Ga; R = CH<sub>3</sub>, SiH<sub>3</sub>, CMe<sub>3</sub>, SiMe<sub>3</sub>), have been investigated at the density functional theory (DFT) level using BP86/TZ2P. The main goals of the present study are (i) to investigate the geometries and to analyze the nature of the M=E bond in the borylene, alylene, and galllyene complexes and (ii) to provide a quantitative differentiation of the M-ER bonds. We will discuss the degree of ionic and covalent character of the M=E bonds as well as the extent of the M → E π back-bonding contribution to the metal-ligand orbital interactions (Figure 1).

## Computational Methods

Calculations of the complexes  $[(\eta^5\text{-C}_5\text{H}_5)(\text{CO})_3\text{M}(\text{ENR}_2)]$  (M = V, E = B, I–IV, R = CH<sub>3</sub>, SiH<sub>3</sub>, CMe<sub>3</sub>, SiMe<sub>3</sub>, E = Al, V–VI, R = CMe<sub>3</sub>, SiMe<sub>3</sub>, E = Ga, VII–VIII, R = CMe<sub>3</sub>, SiMe<sub>3</sub>; M = Nb, E = B, IX–XII, R = CH<sub>3</sub>, SiH<sub>3</sub>, CMe<sub>3</sub>, SiMe<sub>3</sub>, E = Al, XIII–XIV, R = CMe<sub>3</sub>, SiMe<sub>3</sub>, E = Ga, XV–XVI, R = CMe<sub>3</sub>, SiMe<sub>3</sub>) have been performed at the nonlocal DFT level of theory using the exchange functional of Becke<sup>65</sup> and the correlation functional of Perdew<sup>66</sup> (BP86). Scalar relativistic effects have been considered using the ZORA formalism.<sup>67</sup> Uncontracted Slater-type orbitals (STOs) using triple-ξ basis sets augmented by two sets of polarization functions were employed for self-consistent-field (SCF) calculations.<sup>68</sup> The (1s)<sup>2</sup> core electrons of boron, carbon, nitrogen, and oxygen, (1s2s2p)<sup>10</sup> core electrons of vanadium, and

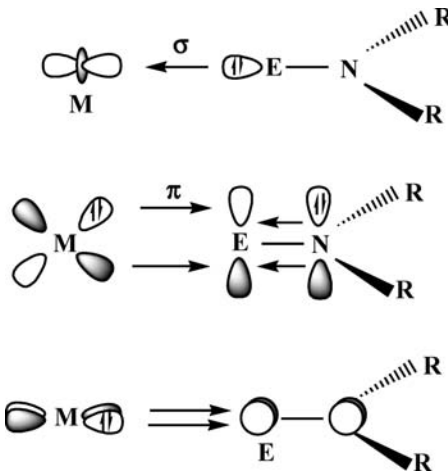


**Figure 1.** Schematic representation of the M-ENR<sub>2</sub> orbital interactions.

(1s2s2p3s3p3d)<sup>28</sup> core electrons of niobium were treated by the frozen-core approximation.<sup>69</sup> An auxiliary set of s, p, d, f, and g STOs was used to fit the molecular densities and to present the Coulomb and exchange potentials accurately in each SCF cycle.<sup>70</sup> Calculations were performed utilizing the program package *ADF-2009.01*.<sup>71</sup>

The binding interactions in complexes I–XVI between the metal fragments  $[(\eta^5\text{-C}_5\text{H}_5)(\text{CO})_3\text{M}]$  (singlet state) and ER fragments [ENR<sub>2</sub>] (singlet state) have been analyzed with  $C_s$  symmetry using the energy decomposition scheme of *ADF*, which is based on the methods of Morokuma<sup>72</sup> and Ziegler and Rauk.<sup>73</sup> The bond energy  $\Delta E$  between fragments is separated into two major components,  $\Delta E_{\text{int}}$  and  $\Delta E_{\text{prep}}$ :

$$\Delta E = \Delta E_{\text{int}} + \Delta E_{\text{prep}} \quad (1)$$

Here,  $\Delta E_{\text{prep}}$  is the energy required to promote the structures of the free fragments from their equilibrium structure in the electronic ground state to the geometry and electronic state that they take up in the molecule:

$$\Delta E_{\text{prep}} = E_{\text{total}}(\text{distorted fragments})$$

$$- E_{\text{total}}(\text{fragments in the equilibrium structure}) \quad (2)$$

$\Delta E_{\text{int}}$  in eq 1 is the instantaneous interaction energy between the two fragments in the molecule. It can be decomposed into three main components:

$$\Delta E_{\text{int}} = \Delta E_{\text{elstat}} + \Delta E_{\text{Pauli}} + \Delta E_{\text{orb}} \quad (3)$$

$\Delta E_{\text{elstat}}$  describes the classical Coulomb interaction between the fragments, which is attractive in most cases. The term

(69) Baerends, E. J.; Autschbach, J. A.; Berces, A.; Bo, C.; Boerriger, P. M.; Cavallo, L.; Chong, D. P.; Deng, L.; Dickson, R. M.; Ellis, D. E.; Fan, L.; Fischer, T. H.; Fonseca Guerra, C.; van Gisbergen, S. J. A.; Groeneweld, J. A.; Gritsenko, O. V.; Grüning, M.; Harris, F. E.; van den Hoek, P.; Jacobsen, H.; van Kessel, G.; Kootstra, F.; van Lenthe, E.; Osinga, V. P.; Patchkovskii, S.; Philipsen, P. H. T.; Post, D.; Pye, C. C.; Ravenek, W.; Ros, P.; Schipper, P. R. T.; Schreckenbach, G.; Snijders, J. G.; Sola, M.; Swart, M.; Swerhone, D.; te Velde, G.; Vernooij, P.; Versluis, L.; Visser, O.; Wezenbeek, E.; Wiesenekker, G.; Wolff, S. K.; Woo, T. K.; Ziegler, T. *ADF 2008-01*; Scientific Computing & Modelling NV: Amsterdam, The Netherlands.

(70) (a) Morokuma, K. *J. Chem. Phys.* **1971**, 55, 1236. (b) Morokuma, K. *Acc. Chem. Res.* **1977**, 10, 294.

(71) (a) Ziegler, T.; Rauk, A. *Theor. Chim. Acta* **1977**, 46, 1. (b) Ziegler, T.; Rauk, A. *Inorg. Chem.* **1979**, 18, 1558. (c) Ziegler, T.; Rauk, A. *Inorg. Chem.* **1979**, 18, 1755.

(72) Pandey, K. K. *Coord. Chem. Rev.* **2009**, 293, 37.

(73) Pandey, K. K.; Lledós, A. *Inorg. Chem.* **2009**, 48, 2748.

- (52) Radius, U.; Bickelhaupt, F. M.; Ehlers, A. W.; Goldberg, N.; Hoffmann, R. *Inorg. Chem.* **1998**, 37, 1080.
- (53) Macdonald, C. L. B.; Cowley, A. H. *J. Am. Chem. Soc.* **1999**, 121, 12113.
- (54) Boehme, C.; Frenking, G. *Chem.—Eur. J.* **1999**, 5, 2184.
- (55) Uddin, J.; Boehme, C.; Frenking, G. *Organometallics* **2000**, 19, 571.
- (56) Chen, Y.; Frenking, G. *Dalton Trans.* **2001**, 434.
- (57) Uddin, J.; Frenking, G. *J. Am. Chem. Soc.* **2001**, 123, 1683.
- (58) Bollwein, T.; Brothers, P. J.; Hermann, H. L.; Schwerdtfeger, P. *Organometallics* **2002**, 21, 5236.
- (59) Boehme, C.; Uddin, J.; Frenking, G. *Coord. Chem. Rev.* **2000**, 197, 249.
- (60) Frenking, G.; Fröhlich, N. *Chem. Rev.* **2000**, 100, 717.
- (61) (a) Frenking, G.; Wichmann, K.; Fröhlich, N.; Loschen, C.; Lein, M.; Frunzke, J.; Rayon, V. M. *Coord. Chem. Rev.* **2003**, 238, 55. (b) Gámez, J. A.; Tonner, R.; Frenking, G. *Organometallics* **2010**, 29, 5676.
- (62) Aldridge, S.; Rossin, A.; Coombs, D. L.; Wilcock, D. J. *Dalton Trans.* **2004**, 2649.
- (63) Pandey, K. K.; Lledós, A.; Maseras, F. *Organometallics* **2009**, 28, 6442.
- (64) Pandey, K. K.; Musaev, D. J. *Organometallics* **2010**, 29, 142.
- (65) (a) Chang, C.; Pelissier, M.; Durand. *Ph. Phys. Scr.* **1986**, 34, 394.
- (b) Heully, J.-L.; Lindgren, I.; Lindroth, E.; Lundquist, S.; Martensson-Pendrill, A.-M. *J. Phys. B* **1986**, 19, 2799. (c) van Lenthe, E.; Baerends, E. J.; Snijders, J. G. *J. Chem. Phys.* **1993**, 99, 4597. (d) van Lenthe, E.; Baerends, E. J.; Snijders, J. G. *J. Chem. Phys.* **1996**, 105, 6505. (e) van Lenthe, E.; van Leeuwen, R.; Baerends, E. J.; Snijders, J. G. *Int. J. Quantum Chem.* **1996**, 57, 281. (f) van Lenthe, E.; Ehlers, A. E.; Baerends, E. J. *J. Chem. Phys.* **1999**, 110, 8943.
- (66) Snijders, J. G.; Baerends, E. J.; Vernooij, P. *At. Data Nucl. Data Tables* **1982**, 26, 483.
- (67) Baerends, E. J.; Ellis, D. E.; Ros, P. *Chem. Phys.* **1973**, 2, 41.
- (68) Krijn, J.; Baerends, E. J. *Fit Functions in the HFS-Method, Internal Report (in Dutch)*; Vrije Universiteit: Amsterdam, The Netherlands, 1984.

$\Delta E_{\text{Pauli}}$ , which is called the exchange repulsion or Pauli repulsion, takes into account the destabilizing two-orbital, three- or four-electron interactions between occupied orbitals of both fragments.  $\Delta E_{\text{Pauli}}$  is calculated by enforcing the Kohn–Sham determinant of the molecule, which results from superimposing both fragments, to obey the Pauli principle through antisymmetrization and renormalization. The last term in eq 3,  $\Delta E_{\text{orb}}$ , gives the stabilizing orbital interactions between occupied and virtual orbitals of the two fragments.  $\Delta E_{\text{orb}}$  can be further partitioned into contributions by the orbitals that belong to different irreducible representations of the point group of the system. It has been suggested that the covalent and electrostatic character of a bond is given by the ratio  $\Delta E_{\text{elstat}}/\Delta E_{\text{orb}}$ .<sup>61,62,74–76</sup> The electronic structures of the complexes were examined by natural bond order (NBO) analysis.<sup>77</sup> All molecular orbital pictures were made by using the MOLDEN program.<sup>78</sup>

## Results and Discussion

**Geometries.** The important optimized bond distances and angles of the complexes  $[(\eta^5\text{-C}_5\text{H}_5)(\text{CO})_3\text{M}(\text{ENR}_2)]$  ( $\text{M} = \text{V}$ ,  $\text{E} = \text{B}$ , **I**–**IV**,  $\text{R} = \text{CH}_3$ ,  $\text{SiH}_3$ ,  $\text{CMe}_3$ ,  $\text{SiMe}_3$ ,  $\text{E} = \text{Al}$ , **V**–**VI**,  $\text{R} = \text{CMe}_3$ ,  $\text{SiMe}_3$ ,  $\text{E} = \text{Ga}$ , **VII**–**VIII**,  $\text{R} = \text{CMe}_3$ ,  $\text{SiMe}_3$ ,  $\text{M} = \text{Nb}$ ,  $\text{E} = \text{B}$ , **IX**–**XII**,  $\text{R} = \text{CH}_3$ ,  $\text{SiH}_3$ ,  $\text{CMe}_3$ ,  $\text{SiMe}_3$ ,  $\text{E} = \text{Al}$ , **XIII**–**XIV**,  $\text{R} = \text{CMe}_3$ ,  $\text{SiMe}_3$ ,  $\text{E} = \text{Ga}$ , **XV**–**XVI**,  $\text{R} = \text{CMe}_3$ ,  $\text{SiMe}_3$ ) at the BP86/TZ2P level are presented in Table 2. The optimized geometries of niobium complexes (**XI**–**XVI**) are shown in Figure 2.

Niobium borylene, alylene, and gallylene complexes are not known so far. We report here for first time the optimized geometries of these niobium complexes (**IX**–**XVI**) as well as of the vanadium complexes  $[(\eta^5\text{-C}_5\text{H}_5)(\text{CO})_3\text{V}(\text{ENR}_2)]$  (**I**–**III** and **V**–**VIII**). Therefore, we cannot compare the calculated values for studied niobium complexes with experimental data. The structural data for the known transition-metal borylene and gallylene complexes were reported (see Table 1). The calculated geometrical parameters of the vanadium borylene complex  $[(\eta^5\text{-C}_5\text{H}_5)(\text{CO})_3\text{V}\{\text{BN}(\text{SiMe}_3)_2\}]$  are in excellent agreement with available experimental values.<sup>5</sup> We expect the same accuracy for the other studied metal borylene, alylene, and gallylene complexes. Variations of the M–E bond distances are presented in Figure S1 in the Supporting Information.

As seen in Table 2, the M–B bond distances in complexes  $[(\eta^5\text{-C}_5\text{H}_5)(\text{CO})_3\text{M}(\text{BNR}_2)]$  ( $\text{M} = \text{V}$ ,  $\text{Nb}$ ;  $\text{R} = \text{Me}$ ,  $\text{SiH}_3$ ,  $\text{CMe}_3$ ,  $\text{SiMe}_3$ ) are longer than those expected for M=B double bonds estimated on the basis of double-bond covalent radii predictions ( $\text{V}=\text{B}$ , 1.90 Å;  $\text{Nb}=\text{B}$ , 2.03 Å).<sup>79</sup> However, the sums of the corresponding M–B single-bond radii amount to  $\text{V}-\text{B}$ , 2.19 Å, and  $\text{Nb}-\text{B}$ , 2.32 Å, respectively.<sup>79</sup> It can be inferred from these observations that the M–B bonds in the borylene complexes **I**–**IV** and **IX**–**XII** have partial M–B double-bond character. Furthermore, the nature of the substituent R of

ligand  $\text{BNR}_2$  has a significant effect on the nature of the M–BNR<sub>2</sub> bonding (Figure S1 in the Supporting Information), as indicated, e.g., by the M–B bond distances, which increase on going from Me to CMe<sub>3</sub> and from SiH<sub>3</sub> to SiMe<sub>3</sub> but decrease on going from CMe<sub>3</sub> to SiMe<sub>3</sub>. In detail, the substituent at nitrogen in ENR<sub>2</sub> [E = B, Al, Ga; R = Me, SiH<sub>3</sub>, C(Me<sub>3</sub>), Si(Me<sub>3</sub>)] species exerts effects on (i) the strength of the M–E bonds, (ii) the charges on metal  $[(\eta^5\text{-C}_5\text{H}_5)(\text{CO})_3\text{M}]$  ( $\text{M} = \text{V}$ , Nb) as well as on ENR<sub>2</sub> fragments, and (iii) the nature of ionic and covalent interactions between these two fragments. In the following, this is exemplified for borylene complexes, based on the nature and properties of the highest occupied molecular orbitals (HOMOs) and lowest unoccupied molecular orbitals (LUMOs) of the corresponding moieties  $[(\eta^5\text{-C}_5\text{H}_5)(\text{CO})_3\text{M}]$  ( $\text{M} = \text{V}$ , Nb) and  $[\text{BNR}_2]$  [R = Me, SiH<sub>3</sub>, C(Me<sub>3</sub>), Si(Me<sub>3</sub>)]. The energies of the HOMOs and LUMOs of the metal fragments vary as  $[(\eta^5\text{-C}_5\text{H}_5)(\text{CO})_3\text{V}]$  (HOMO, −4.934 eV; LUMO, −4.155 eV) and  $[(\eta^5\text{-C}_5\text{H}_5)(\text{CO})_3\text{Nb}]$  (HOMO, −4.873 eV; LUMO, −4.002 eV), while the corresponding energies of the  $[\text{BNR}_2]$  species are calculated as  $[\text{BNMe}_2]$  (HOMO, −4.968 eV; LUMO, −2.026 eV),  $[\text{BN}(\text{SiH}_3)_2]$  (HOMO, −5.352 eV; LUMO, −2.090 eV),  $[\text{BN}(\text{CMe}_3)_2]$  (HOMO, −4.286 eV; LUMO, −1.226 eV), and  $[\text{BN}(\text{SiMe}_3)_2]$  (HOMO, −4.566 eV; LUMO, −1.241 eV). Evidently, the LUMO of the metal fragments  $[(\eta^5\text{-C}_5\text{H}_5)(\text{CO})_3\text{M}]$  is closer in energy to the HOMO of  $[\text{BN}(\text{CMe}_3)_2]$  (as an example) than to the HOMO of  $[\text{BNMe}_2]$ , allowing for relatively better ligand-to-metal donation and thus, slightly stronger M–B σ-bond interaction in  $[(\eta^5\text{-C}_5\text{H}_5)(\text{CO})_3\text{M}\{\text{BN}(\text{CMe}_3)_2\}]$ . On the other hand, the HOMO of the metal fragments  $[(\eta^5\text{-C}_5\text{H}_5)(\text{CO})_3\text{M}]$  is closer in energy to the LUMO of  $[\text{BNMe}_2]$  than to the LUMO of the  $[\text{BN}(\text{CMe}_3)_2]$  ligand, resulting in better metal-to-ligand π back-bonding. The latter effect appears to outweigh the aforementioned σ-bond interaction, and thus, as a net effect, a lengthening of the M–B bond in  $[(\eta^5\text{-C}_5\text{H}_5)(\text{CO})_3\text{M}\{\text{BN}(\text{CMe}_3)_2\}]$  is observed in comparison to that in  $[(\eta^5\text{-C}_5\text{H}_5)(\text{CO})_3\text{M}\{\text{BNMe}_2\}]$ .

The optimized B–N bond distances (1.384–1.395 Å) in the metal borylene complexes **I**–**IV** and **IX**–**XII** are similar to those expected for double bonds based on covalent radii predictions (B=N, 1.38 Å)<sup>79</sup> and are shorter than those expected for single bonds based on covalent radii predictions (B–N, 1.55 Å).<sup>80</sup> The results reveal that the B–N linkages in the metal borylene complexes represent nearly B=N double bonds.

The M–E bond distances ( $\text{V}-\text{Al} = 2.406$  Å in **V** and 2.398 Å in **VI**;  $\text{V}-\text{Ga} = 2.398$  Å in **VII** and 2.384 Å in **VIII**;  $\text{Nb}-\text{Al} = 2.556$  Å in **XIII** and 2.530 Å in **XIV**;  $\text{Nb}-\text{Ga} = 2.538$  Å in **XV** and 2.526 Å in **XVI**) in the studied metal alylene and gallylene complexes almost resemble those expected for a single bond based on covalent radii predictions ( $\text{V}-\text{Al}$ , 2.40 Å;  $\text{V}-\text{Ga}$ , 2.44 Å;  $\text{Nb}-\text{Al}$ , 2.52 Å;  $\text{Nb}-\text{Ga}$ , 2.56 Å) and are significantly larger than the sum of the double-bond covalent radii ( $\text{V}=\text{Al}$ , 2.25 Å,  $\text{V}=\text{Ga}$ , 2.29 Å,  $\text{Nb}=\text{Al}$ , 2.38 Å,  $\text{Nb}=\text{Ga}$ , 2.42 Å).<sup>79</sup> Thus, the M–E bonds in the studied metal alylene and gallylene complexes represent M–E single bonds with very small M–E π-orbital contribution (see Figure S1 in the Supporting Information and Table 4). The optimized Al–N and Ga–N bond distances ( $\text{Al}-\text{N}$ , 1.806–1.823 Å;  $\text{Ga}-\text{N}$ , 1.864–1.875 Å) in the metal alylene and gallyne

(74) Pandey, K. K.; Patidar, P.; Braunschweig, H. *Inorg. Chem.* **2010**, *49*, 6994.

(75) Reed, A. E.; Curtiss, L. A.; Weinhold, F. *Chem. Rev.* **1988**, *88*, 899.

(76) Schaftenaar, G. *MOLDEN3.4*; CAOS/CAMM Center: Nijmegen, The Netherlands, 1998.

(77) Pykkö, P.; Atsumi, M. *Chem.—Eur. J.* **2009**, *15*, 12770.

(78) (a) Wells, A. F. *Structural Inorganic Chemistry*, 5th ed.; Clarendon: Oxford, U.K., 1984. (b) Pauling, L. *The Nature of the Chemical Bond*, 3rd ed.; Cornell University Press: Ithaca, NY, 1960.

(79) Wiberg, K. B. *Tetrahedron* **1968**, *24*, 1083.

**Table 2.** Selected Optimized Geometrical Parameters for Neutral Terminal Borylene, Altylene, and Galliylene Complexes [ $\eta^5\text{-C}_5\text{H}_5(\text{CO})_3\text{M}(\text{ENR}_2)$ ] (**I**–**XVI**; M = V, Nb; E = B, Al, Ga; R = CH<sub>3</sub>, SiH<sub>3</sub>, CM<sub>3</sub>, SiMe<sub>3</sub>)<sup>a</sup>

R =	[(Cp)(CO) <sub>3</sub> V(BNR <sub>2</sub> )]				[(Cp)(CO) <sub>3</sub> V(AlNR <sub>2</sub> )]				[(Cp)(CO) <sub>3</sub> V(GaNR <sub>2</sub> )]				[(Cp)(CO) <sub>3</sub> Nb(AlNR <sub>2</sub> )]				[(Cp)(CO) <sub>3</sub> Nb(GaNR <sub>2</sub> )]				
	Me ( <b>I</b> )	SiH <sub>3</sub> ( <b>II</b> )	CM <sub>3</sub> ( <b>III</b> )	SiMe <sub>3</sub> ( <b>IV</b> )	[(Cp)(CO) <sub>3</sub> V(SiMe <sub>3</sub> )]				[(Cp)(CO) <sub>3</sub> V(CMe <sub>3</sub> )]				[(Cp)(CO) <sub>3</sub> V(Me)]				[(Cp)(CO) <sub>3</sub> Nb(SiMe <sub>3</sub> )]				
					CMe <sub>3</sub> ( <b>V</b> )	SiMe <sub>3</sub> ( <b>VI</b> )	SiMe <sub>3</sub> ( <b>VII</b> )	SiMe <sub>3</sub> ( <b>VIII</b> )	Me ( <b>IX</b> )	SiH <sub>3</sub> ( <b>X</b> )	CMe <sub>3</sub> ( <b>XI</b> )	SiMe <sub>3</sub> ( <b>XII</b> )	CM <sub>3</sub> ( <b>XIII</b> )	SiMe <sub>3</sub> ( <b>XIV</b> )	SiMe <sub>3</sub> ( <b>XV</b> )	SiMe <sub>3</sub> ( <b>XVI</b> )	[(Cp)(CO) <sub>3</sub> Nb(GaNR <sub>2</sub> )]				
Bond Distances																					
M–E	1.949	1.945	2.013	1.991	1.959(6) <sup>b</sup>	2.406	2.379	2.398	2.384	2.098	2.099	2.170	2.153	2.556	2.530	2.538	2.526				
M–E Pauling Bond Order																					
E–N	(1.34)	(1.36)	(1.09)	(1.17)	(1.00)	(1.07)	(1.15)	(1.20)	(1.22)	(1.00)	(1.02)	(0.89)	(0.97)						(1.07)	(1.12)	
	1.384	1.395	1.395	1.384	1.384	1.823	1.806	1.875	1.864	1.380	1.391	1.391	1.378	1.820	1.807	1.875	1.864				
N–C	1.466	1.54	1.788	1.828	1.496	1.781	1.495	1.780	1.466	1.786	1.539	1.496	1.496						1.495		
N–Si	1.894	1.891	1.894	1.889	1.907	1.907	1.916	1.917	2.099	2.048	2.052	2.049	2.049	1.779	1.779	1.779	1.778				
M–CO <sup>c</sup>	1.921	1.926	1.919	1.917	1.906	1.908	1.905	1.908	2.077	2.082	2.077	2.082	2.082	2.058	2.058	2.058	2.066	2.066	2.065	2.065	
C–O <sup>c</sup>	1.181	1.180	1.175	1.176	1.178	1.179	1.173	1.173	1.747	1.849	1.747	1.849	1.849	2.075	2.075	2.075	2.075	2.075	2.063	2.063	
	1.162	1.16	1.164	1.163	1.166	1.166	1.166	1.165	1.161	1.160	1.163	1.163	1.163	1.164	1.164	1.164	1.164	1.164	1.163	1.163	
Bond Angles																					
M–E–N	178.1	179.2	174.9	176.7	176.5	174.4	178.6	176.7	179.7	179.6	175.5	176.6	176.5	174.6	174.6	174.6	174.6	174.6	178.6	178.8	
C–E–C	114.3	125.3	119.8	126	124.6	125.1	124.6	125.1	114.8	126.2	120.5	126.2	124.8						124.8		
Si–E–Si	62.7	62.4	72.4	68.5	71.5	69.9	74.4	74.0	62.6	72.4	73.6	69.9	69.9	127.5	127.5	127.5	127.5	127.5	126.0	126.4	
E–M–CO <sup>c</sup>	112.7	112.4	122.9	118.4	120.4	118.4	123.0	122.1	109.2	109.1	119.4	115.7	116.2	68.5	68.5	68.5	68.5	68.5	72.9	72.9	

<sup>a</sup>Distances are in angstroms, and angles are in degrees. <sup>b</sup>X-ray structure data for [ $\eta^5\text{-C}_5\text{H}_5(\text{CO})_3\text{V}\{\text{BN}(\text{SiMe}_3)_2\}]^5$ . Cp =  $\eta^5\text{-C}_5\text{H}_5$ . <sup>c</sup>The first value refers to the CO groups syn to ENR<sub>2</sub>, and the second value refers to the trans CO ligand.

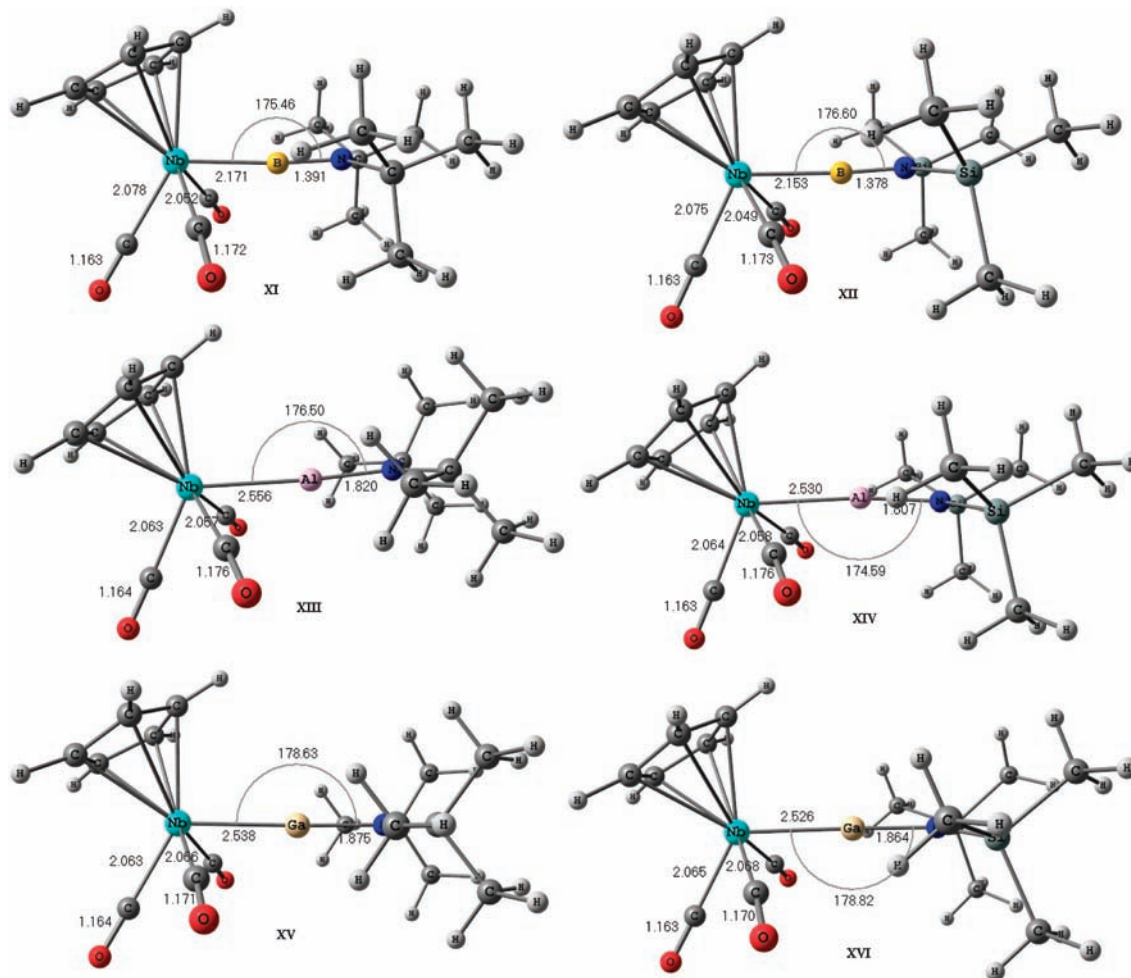


**Figure 2.** Optimized geometries of niobium borylene, alylene, and gallylene complexes  $[(\eta^5\text{-C}_5\text{H}_5)(\text{CO})_3\text{Nb}(\text{ENR}_2)]$ . The important bond lengths and angles are given in Table 2.

complexes **V–VIII** and **XIII–XVI** are shorter than expected for a single bond based on covalent radii predictions (Al–N, 1.91 Å; Ga–N, 1.95 Å) and longer than those expected for a double bond based on covalent radii predictions (Al=N, 1.73 Å; Ga=N, 1.77 Å).<sup>79</sup> Thus, the Al–N and Ga–N bonds in the complexes **V–VIII** and **XIII–XVI** have partial double-bond character. The M–E–N bond angles in **I–XVI** deviate slightly from linearity.

**Bonding Analysis of M–ENR<sub>2</sub> Bonds.** We start the analysis of the bonding situation of M–E bonds in the borylene, alylene, and gallylene complexes **I–XVI** with a discussion of bond orders and atomic charges. Table 3 gives the Wiberg bond indices (WBIs)<sup>79</sup> and natural population analysis (NPA) charges.

Table 3 shows that the WBI values of the M–E bonds in the vanadium complexes  $[(\eta^5\text{-C}_5\text{H}_5)(\text{CO})_3\text{V}(\text{ENR}_2)]$  (**I–VIII**) are smaller than the corresponding WBI values of the M–E bonds in the niobium complexes  $[(\eta^5\text{-C}_5\text{H}_5)(\text{CO})_3\text{Nb}(\text{BNR}_2)]$  (**IX–XVI**). The results reveal the expected periodic trend in the bond strengths due to the d-orbital extent. The WBI values of the M–Al and M–Ga bonds (~0.50) in the alylene and gallylene complexes are significantly lower than the WBI values of the M–B bonds (~1.0). Similar results are found for the E–N bonds (Table 3). One can infer from these observations that

there is multiple-bond character in the V–B–N moiety in the metal borylene complexes **I–IV** and **IX–XII**, while relatively poor M–E  $\sigma$  and  $\pi$  bonding is present in metal alylene and gallylene complexes. The WBI values of the M–CO bonds indicate that the CO ligand trans to the ENR<sub>2</sub> moiety is more weakly bound than the CO ligands in the cis position because of the enhanced trans effect of the ENR<sub>2</sub> ligands.<sup>8,51,55</sup> The calculated NPA charge distributions indicate that the metal atoms carry negative charges and the boron, aluminum, and gallium atoms carry significantly larger positive charges in the complexes **I–XVI**. On going from vanadium to niobium, the negative charge on the metal decreases significantly. The energy increase for  $d_{\pi}(\text{HOMO})$  (as mentioned earlier) of the  $[(\eta^5\text{-C}_5\text{H}_5)(\text{CO})_3\text{Nb}]$  fragment will enhance  $\pi$  back-donation to the [BNR<sub>2</sub>] species because this orbital is closer in energy to the LUMO of [BNR<sub>2</sub>]. Because of the relatively greater  $\pi$  back-donation from  $[(\eta^5\text{-C}_5\text{H}_5)(\text{CO})_3\text{Nb}]$  to [BNR<sub>2</sub>] than from  $[(\eta^5\text{-C}_5\text{H}_5)(\text{CO})_3\text{V}]$  to [BNR<sub>2</sub>], the charge on niobium is less negative. Additionally, the larger polarization of the electronic charge toward C<sub>5</sub>H<sub>5</sub> in the niobium complexes may also be held responsible for the smaller negative charge on niobium than on vanadium. It is surprising to note that CH<sub>3</sub> and SiH<sub>3</sub> are observed to be better donors than CMe<sub>3</sub> and SiMe<sub>3</sub>.

**Table 3.** WBIs, NPA Charges, and Results of the NBO Analysis for Neutral Terminal Borylene, Alkyne, and Gallylene Complexes [ $(\eta^5\text{-C}_5\text{H}_5)(\text{CO})_3\text{M}(\text{ENR}_2)$ ] (**I**–**XVI**; M = V, Nb; E = B, Al, Ga; R =  $\text{CH}_3$ ,  $\text{SiH}_3$ ,  $\text{CM}_{\text{E}_3}$ ,  $\text{SiMe}_3$ )

R =	[(Cp)(CO) <sub>3</sub> V(BNR <sub>2</sub> )]			[(Cp)(CO) <sub>3</sub> V(GaNR <sub>2</sub> )]			[(Cp)(CO) <sub>3</sub> Nb(BNR <sub>2</sub> )]			[(Cp)(CO) <sub>3</sub> Nb(AINR <sub>2</sub> )]		
	Me ( <b>I</b> )	SiH <sub>3</sub>	CMe <sub>3</sub>	SiMe <sub>3</sub> ( <b>IV</b> )	CMe <sub>3</sub> ( <b>V</b> )	SiMe <sub>3</sub> ( <b>VI</b> )	CMe <sub>3</sub> ( <b>VII</b> )	SiMe <sub>3</sub> ( <b>VIII</b> )	Me ( <b>IX</b> )	SiH <sub>3</sub>	CMe <sub>3</sub>	SiMe <sub>3</sub> ( <b>XII</b> )
		SiH <sub>3</sub> ( <b>II</b> )	CMe <sub>3</sub> ( <b>III</b> )	SiMe <sub>3</sub> ( <b>IV</b> )		SiH <sub>3</sub> ( <b>X</b> )			SiH <sub>3</sub> ( <b>X</b> )	CMe <sub>3</sub> ( <b>XI</b> )	SiMe <sub>3</sub> ( <b>XIII</b> )	CM <sub>E</sub> <sub>3</sub> ( <b>XIV</b> )
WBIs												
M–E	0.79	0.80	0.82	0.79	0.60	0.64	0.65	0.96	0.97	0.99	0.95	0.68
E–N	1.03	1.03	0.94	1.07	0.55	0.47	0.58	0.49	1.02	1.07	0.95	0.55
M–C(CO) <sup>a</sup>	1.02	1.01	1.00	1.02	1.12	1.07	1.02	1.03	1.08	1.07	1.06	1.12
C–O <sup>a</sup>	0.91	0.90	0.91	0.92	1.01	0.93	0.96	0.94	0.97	0.96	0.98	1.01
C <sub>5</sub> H <sub>5</sub>	1.95	1.99	1.97	1.96	2.01	1.97	2.01	2.01	1.95	1.99	1.98	1.96
ENR <sub>2</sub>	2.12	2.13	2.10	2.11	2.08	2.10	2.08	2.09	2.10	2.09	2.08	2.10
CO <sup>a</sup>	0.09	0.10	0.14	0.12	0.04	0.02	0.10	0.09	−0.03	−0.02	0.01	−0.07
CO <sup>b</sup>	0.24	0.25	0.24	0.24	0.21	0.22	0.20	0.21	0.11	0.20	0.11	0.09
NPA Charges												
M	−1.06	−1.07	−1.20	−1.16	−1.23	−1.23	−1.19	−1.20	−0.30	−0.41	−0.38	−0.56
E	0.88	0.88	0.95	0.92	1.39	1.55	1.17	1.31	0.77	0.78	0.78	1.32
C <sub>5</sub> H <sub>5</sub>	0.05	0.07	0.08	0.07	0.06	0.08	0.07	0.09	−0.22	−0.20	−0.21	−0.19
ENR <sub>2</sub>	0.59	0.55	0.60	0.61	0.88	0.89	0.72	0.72	0.47	0.34	0.48	0.47
CO <sup>a</sup>	0.24	0.25	0.24	0.24	0.21	0.22	0.20	0.21	0.11	0.20	0.11	0.11
CO <sup>b</sup>	0.24	0.25	0.24	0.24	0.21	0.22	0.20	0.21	0.11	0.20	0.11	0.09

<sup>a</sup>The first value refers to the CO groups syn to ENR<sub>2</sub>, and the second value refers to the trans CO ligand.

**Table 4.** EDA<sup>a</sup> of Neutral Terminal Borylene, Alkyne, and Gallylene Complexes [ $(\eta^5\text{-C}_5\text{H}_5)(\text{CO})_3\text{M}(\text{ENR}_2)$ ] (**I**–**XVI**; M = V, Nb; E = B, Al, Ga; R =  $\text{CH}_3$ ,  $\text{SiH}_3$ ,  $\text{CM}_{\text{E}_3}$ ,  $\text{SiMe}_3$ ) at BP86/TZ2P

R =	[(Cp)(CO) <sub>3</sub> V(BNR <sub>2</sub> )]			[(Cp)(CO) <sub>3</sub> V(AINR <sub>2</sub> )]			[(Cp)(CO) <sub>3</sub> Nb(BNR <sub>2</sub> )]			[(Cp)(CO) <sub>3</sub> Nb(AINR <sub>2</sub> )]			[(Cp)(CO) <sub>3</sub> Nb(GaN <sub>2</sub> )]		
	Me ( <b>I</b> )	SiH <sub>3</sub>	CMe <sub>3</sub>	SiMe <sub>3</sub> ( <b>IV</b> )	SiH <sub>3</sub>	CMe <sub>3</sub>	SiMe <sub>3</sub> ( <b>VI</b> )	SiH <sub>3</sub>	CMe <sub>3</sub>	SiMe <sub>3</sub> ( <b>XII</b> )	SiH <sub>3</sub>	CMe <sub>3</sub>	SiMe <sub>3</sub> ( <b>XIV</b> )		
		SiH <sub>3</sub> ( <b>II</b> )	CMe <sub>3</sub> ( <b>III</b> )	SiMe <sub>3</sub> ( <b>IV</b> )	SiH <sub>3</sub> ( <b>X</b> )	CMe <sub>3</sub> ( <b>V</b> )	SiMe <sub>3</sub> ( <b>VII</b> )	Me ( <b>IX</b> )	SiH <sub>3</sub> ( <b>X</b> )	CMe <sub>3</sub> ( <b>XI</b> )	SiMe <sub>3</sub> ( <b>XIII</b> )	CM <sub>E</sub> <sub>3</sub> ( <b>XIV</b> )	CM <sub>E</sub> <sub>3</sub> ( <b>XVI</b> )		
$\Delta E_{\text{int}}$															
$\Delta E_{\text{Pauli}}$	−87.1	−84.4	−76.2	−78.4	−52.6	−51.6	−43.2	−42.2	−85.8	−82.6	−76.8	−77.9	−54.5		
$\Delta E_{\text{electstat}}$	365.3	361.9	237.1	272.6	180.5	188.8	135.2	133.8	296.0	284.0	200.5	216.4	158.7		
$\Delta E_{\pi}^{(a)}$	−239.5	−231.6	−179.2	−195.9	−127.4	−98.6	−55.4	−216.9	−203.2	−167.7	−175.1	−121.9	−120.8		
$\Delta E_{\text{orb}}$	−212.9	−214.7	(51.2%)	(57.2%)	(55.8%)	(54.6%)	(53.5%)	(54.2%)	(56.8%)	(60.5%)	(59.5%)	(59.5%)	(57.2%)		
$\Delta E_{\text{orb}}^{(a)}$	−170.7	−172.0	−105.2	−125.3	−155.2	−105.7	−111.6	−79.8	−80.6	−165.0	−163.4	−109.6	−91.3		
$\Delta E_{\pi}^{(b)}$	−42.3	−42.7	−28.9	−29.9	−12.7	−14.6	−10.4	−69.4	−69.1	−130.3	−129.4	−84.0	−94.6		
$\Delta E_{\text{prep}}$	4.2	4.1	(19.7%)	(21.5%)	(19.3)	(12.0%)	(13.1%)	(14.3%)	(21.1%)	(20.8%)	(23.3%)	(20.6%)	(14.2%)		
$\Delta E_{(-\text{BDE})}$	−82.9	−80.3	−69.1	−72.6	−50.7	−48.1	−41.7	−39.7	−80.8	−76.8	−69.6	−72.2	−52.1		

<sup>a</sup>Energy contributions in kcal/mol. <sup>b</sup>The values in parentheses are the percentage contributions to the total electrostatic interactions, reflecting the ionic character of the bond. <sup>c</sup>The values in parentheses are the percentage contributions of  $\pi$  bonding to the total orbital interactions  $\Delta E_{\text{orb}}$ . Bond dissociation energy with a negative sign. Cp =  $\eta^5\text{-C}_5\text{H}_5$ .

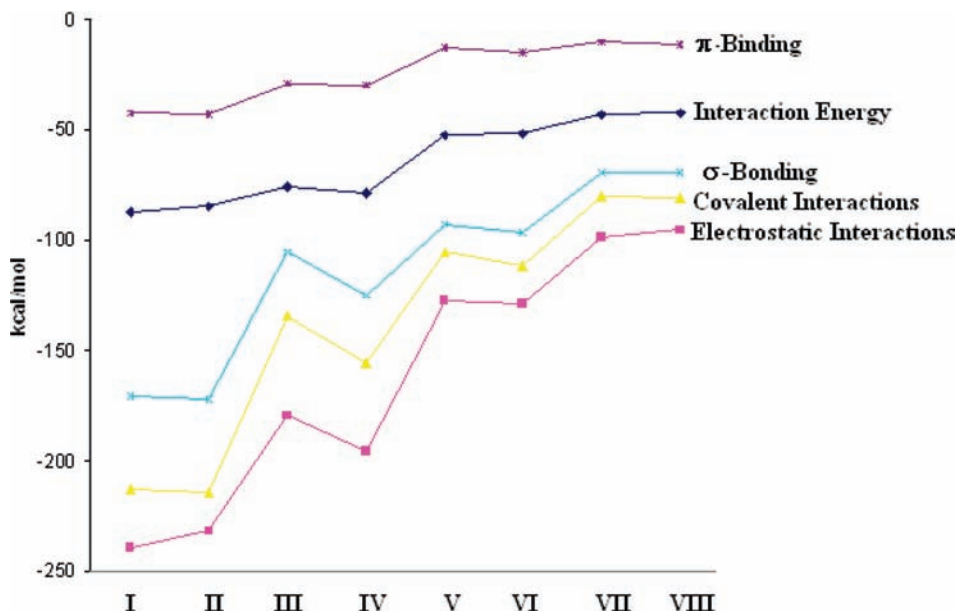


**Figure 3.** Values of the energy contributions of the interaction energy, electrostatic interactions (ionic contribution), orbital interactions (covalent interaction),  $\sigma$  bonding, and  $\pi$  bonding to the V–E bonds in the terminal borylene, alylene, and gallylene complexes of vanadium [ $(\eta^5\text{-C}_5\text{H}_5)(\text{CO})_3\text{V}(\text{ENR}_2)$ ] [E = B and R = Me (**I**), SiH<sub>3</sub> (**II**), CMe<sub>3</sub> (**III**), SiMe<sub>3</sub> (**IV**); E = Al and, R = CMe<sub>3</sub> (**V**), SiMe<sub>3</sub> (**VI**); E = Ga and R = CMe<sub>3</sub> (**VII**), SiMe<sub>3</sub> (**VIII**)]. A negative sign indicates attractive interaction.

**EDA of M–E (E = B, Al, Ga) Bonding.** Besides the charge decomposition analysis using the NBO method, we also performed EDA of the M=E bonds in terminal borylene, alylene, and gallylene complexes **I**–**XVI**. The results are given in Table 4 and Figures S1 and S2 in the Supporting Information. EDA of the neutral borylene and gallylene complexes was reported by Frenking et al.<sup>54–61</sup>

The tabulated bond dissociation energies in Table 4 reveal the expected periodic trend in the bond strengths due to the d-orbital extent: the Nb=E bonds of complexes **XI**–**XVI** are slightly stronger than the V=E bonds of complexes **III**–**VIII**. We observed the opposite trend for better electron-donating ligands CH<sub>3</sub> and SiH<sub>3</sub> (niobium complexes **IX** and **X** vs vanadium complexes **I** and **II**). Figures 3 and S2 in the Supporting Information show a diagram of the  $\pi$ -bonding and  $\sigma$ -bonding interaction energies  $\Delta E_{\text{int}}$ , orbital interaction energies  $\Delta E_{\text{orb}}$ , and electrostatic interactions  $\Delta E_{\text{elstat}}$ . The breakdown of the interaction energy  $\Delta E_{\text{int}}$  into the repulsive term  $\Delta E_{\text{Pauli}}$  and the attractive terms  $\Delta E_{\text{orb}}$  and  $\Delta E_{\text{elstat}}$  shows that the  $\Delta E_{\text{Pauli}}$  repulsive interactions have the larger absolute value for the studied complexes **I**–**XVI** (Table 4). We also note the  $\Delta E_{\text{Pauli}}$  repulsive interactions are larger for vanadium complexes **I**–**VIII** than for niobium complexes **IX**–**XVI**. The differences in the values of the energy terms for niobium complexes compared to those for vanadium complexes are mainly due to the relativistic effects of niobium as well as the nature of the substituents at nitrogen.

The contributions of the electrostatic interaction terms  $\Delta E_{\text{elstat}}$  are larger in all borylene, alylene, and gallylene complexes **I**–**XVI** than the covalent bonding  $\Delta E_{\text{orb}}$  term. Thus, the  $[\text{M}] = \text{BNR}_2$  ( $[\text{M}] = [(\eta^5\text{-C}_5\text{H}_5)(\text{CO})_3\text{M}]$ ) bonds have a greater degree of ionic character (see Figure 3). The results reveal that (1) the nature of the substituent R in ENR<sub>2</sub> has an insignificant effect on the ionic character of the  $[\text{M}] = \text{ENR}_2$  bonds and (2) the ionic character in niobium borylene, alylene, and gallylene complexes is

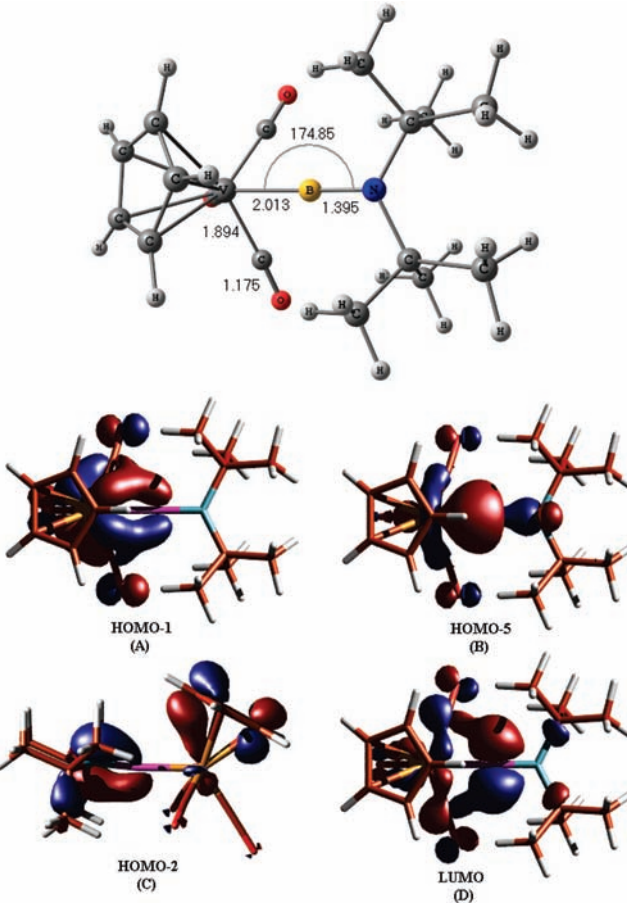


**Figure 4.** Optimized geometry and plot of some relevant orbitals of **III**.

slightly greater than those in the corresponding vanadium complexes. Table 4 also gives the breakdown of the orbital interactions  $\Delta E_{\text{orb}}$  into the  $\text{M} \leftarrow \text{BR}$   $\sigma$ -donation and  $\text{M} \rightarrow \text{BR}$   $\pi$ -back-donation components. It is significant to note

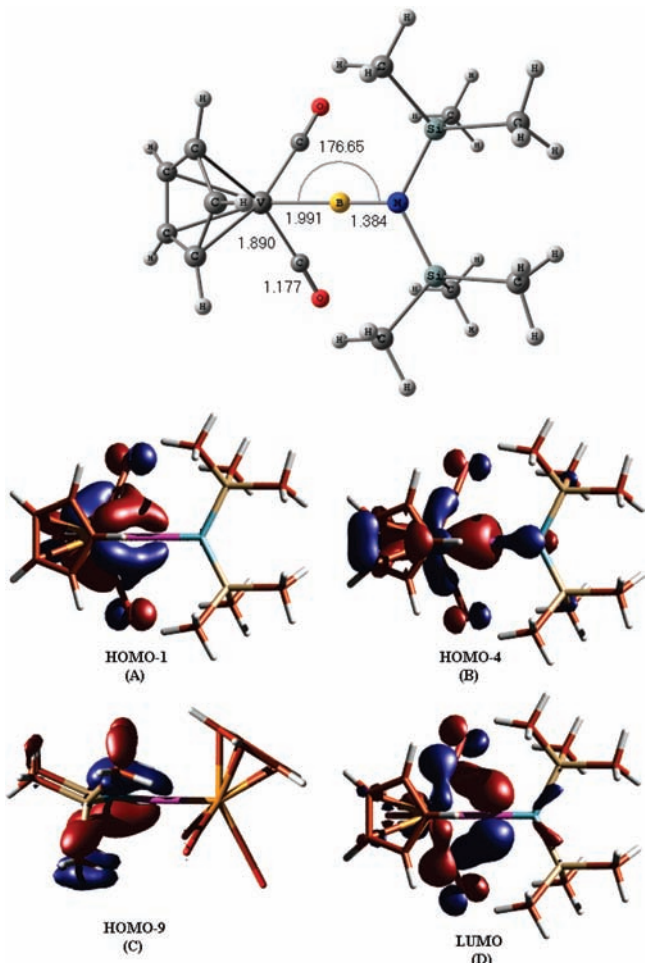


**Figure 5.** Optimized geometry and plot of some relevant orbitals of **IV**.

that the  $\pi$ -bonding contribution in all complexes is smaller (12.0–23.3% of total orbital contributions) than the  $\sigma$ -bonding contribution, and the relatively highest percentage value is found for  $\text{BN}(\text{CMe}_3)_2$  ligands. A relatively larger  $\pi$  contribution is found for the borylene complexes  $[(\eta^5\text{-C}_5\text{H}_5)(\text{CO})_3\text{M}(\text{BNR}_2)]$  than for the alylene complexes  $[(\eta^5\text{-C}_5\text{H}_5)(\text{CO})_3\text{M}(\text{AlNR}_2)]$  and gallylene complexes  $[(\eta^5\text{-C}_5\text{H}_5)(\text{CO})_3\text{M}(\text{BNR}_2)]$ . The trend of variation in all energy terms (interaction energy, electrostatic interaction, orbital contribution,  $\sigma$ -bonding contribution, as well as  $\pi$ -bonding contribution) is  $\text{BNR}_2 > \text{AlNR}_2 > \text{GaNR}_2$ . From the data presented in Table 4, it could be inferred that the  $\text{ENR}_2$  ligands dominantly behave as  $\sigma$  donors.

To visualize the differences in  $\text{M}=\text{B}$  bonding in the borylene complexes, envelope plots of some relevant orbitals of the vanadium complexes  $[(\eta^5\text{-C}_5\text{H}_5)(\text{CO})_3\text{V}\{\text{BN}(\text{CMe}_3)_2\}]$  (**III**) and  $[(\eta^5\text{-C}_5\text{H}_5)(\text{CO})_3\text{V}\{\text{BN}(\text{SiMe}_3)_2\}]$  (**IV**) are given in Figures 4 and 5, respectively. Figure 4A and 5A give a pictorial description of the  $\text{V}-\text{B}$   $\pi$  orbital along with the  $\text{V}-\text{CO}$   $\pi$  orbital, which are very similar (see also Figures 3 and S2 in the Supporting Information). Figures 4B and 5B show  $\text{V}-\text{B}$   $\sigma$  bondings that are quite different, indicating stronger  $\text{V}-\text{B}$   $\sigma$  interaction in complex **IV** than in complex **III**. Figures 4C and 5C give pictorial descriptions of the  $\text{B}-\text{N}$   $\pi$  orbitals. Figures 4D and 5D display boron  $\pi$  orbitals that have some overlap with CO carbon  $\pi$  orbitals. It is important to note that the

latter interaction is greater in complex **IV** than in complex **III**. It is also significant to note that  $\text{V}-\text{Al}$  and  $\text{V}-\text{Ga}$   $\pi$  orbitals in the complexes  $[(\eta^5\text{-C}_5\text{H}_5)(\text{CO})_3\text{V}\{\text{EN}(\text{SiMe}_3)_2\}]$  ( $\text{E} = \text{Al}, \text{Ga}$ ) have very small contributions, with major contributions from the  $\text{V}-\text{CO}$   $\pi$  orbital (see Figure S3 in the Supporting Information).

## Conclusion

From the theoretical studies presented above on the structure and bonding in 16 neutral terminal borylene, alylene, and gallylene complexes of vanadium and niobium, one can draw the following conclusions:

- 1 Here, for the first time (except for the vanadium complex **IV**), we reported the optimized geometry and electronic structure of, as well as analyzed the nature of,  $\text{M}=\text{BNR}_2$  bonds in the terminal neutral metal borylene, alylene, and gallylene complexes of vanadium and niobium  $[(\eta^5\text{-C}_5\text{H}_5)(\text{CO})_3\text{M}(\text{ENR}_2)]$  (where  $\text{M} = \text{V}$  and  $\text{Nb}$  and  $\text{R} = \text{Me}, \text{SiH}_3, \text{CMe}_3$ , and  $\text{SiMe}_3$ ). The calculated geometry parameters of the vanadium borylene complex  $[(\eta^5\text{-C}_5\text{H}_5)(\text{CO})_3\text{V}\{\text{BN}(\text{SiMe}_3)_2\}]$  (**IV**) are in excellent agreement with their available experimental values.<sup>5</sup>
- 2 The  $\text{M}-\text{B}$  bonds in the borylene complexes have partial  $\text{M}-\text{B}$  double-bond character, and the  $\text{B}-\text{N}$  bonds are nearly  $\text{B}=\text{N}$  double bonds. On the other hand, the  $\text{M}-\text{E}$  bonds in the studied metal alylene and gallylene complexes represent  $\text{M}-\text{E}$  single bonds with very small  $\text{M}-\text{E}$   $\pi$ -orbital contribution, and the  $\text{Al}-\text{N}$  and  $\text{Ga}-\text{N}$  bonds in the complexes have partial double-bond character.
- 3 The nature of the substituent  $\text{R}$  of ligand  $\text{BNR}_2$  has a significant effect on the nature of the  $\text{M}-\text{BNR}_2$  bonding:  $\text{M}-\text{B}$  bond distances increase on going from  $\text{Me}$  to  $\text{CMe}_3$  and from  $\text{SiH}_3$  to  $\text{SiMe}_3$  but decrease on going from  $\text{CMe}_3$  to  $\text{SiMe}_3$ .
- 4 The WBI values of the  $\text{M}-\text{Al}$  and  $\text{M}-\text{Ga}$  bonds ( $\sim 0.50$ ) in the alylene and gallylene complexes are significantly lower than the WBI values of the  $\text{M}-\text{B}$  bonds ( $\sim 1.0$ ).
- 5 The orbital interactions between metal and  $\text{ENR}_2$  in  $[(\eta^5\text{-C}_5\text{H}_5)(\text{CO})_3\text{M}(\text{ENR}_2)]$  arise mainly from  $\text{M} \leftarrow \text{ENR}_2$   $\sigma$  donation. In all studied complexes, the  $\pi$ -bonding contribution to the total  $\text{M}-\text{ENR}_2$  bond is significantly smaller than that of the  $\sigma$ -bonding contribution and decreases upon going from  $\text{M} = \text{V}$  to  $\text{Nb}$ . Thus, in the  $\text{ENR}_2$  ligand, boron, aluminum, and gallium dominantly behave as  $\sigma$  donors. The contributions of the electrostatic interactions  $\Delta E_{\text{elstat}}$  are significantly larger in all borylene, alylene, and gallylene complexes than the covalent bonding  $\Delta E_{\text{orb}}$ ; that is, the  $[\text{M}]-\text{BNR}_2$  bonding in the complexes has a greater degree of ionic character.

**Acknowledgment.** K.K.P. acknowledges Alexander von Humboldt Foundation, Germany, for a fellowship.

**Supporting Information Available:** Cartesian coordinates of the optimized geometries of terminal metal borylene, alylene, and gallylene complexes (**I–XVI**) and relevant molecular orbitals of **VI** and **VIII**. This material is available free of charge via the Internet at <http://pubs.acs.org>.